Towards an Automatic Vehicle Access Control System: License Plate Location

Pedro R. Mendes Júnior, José M. R. Neves, Andréa I. Tavares, David Menotti
Computing Department
Federal University of Ouro Preto (UFOP)
Ouro Preto, Minas Gerais, Brazil
{pedrormjunior, jmrneves, andrea.iabrudi, menottid}@gmail.com

***Abstract*—An automatic vehicle access control system (AVACS) can be divided into three steps: vehicle location, vehicle license plate (VLP) location, and VLP recognition. This paper presents a new method for VLP location based on the horizontal gradient, morphological operations, connected components analysis, and statistical measures. First, the horizontal gradient is acquired and a mean filter is applied on it. Morphological operations are then used to darken non-VLP high-valued regions (saliences). At this step, we work on an integer-valued image rather than on the binary one, improving salience detection. Finally, the image is binarized, then a connected component analysis is performed, and statistical measures are used to decide among the VLP candidates. Experiments show that, in a database of 722 images, our method correctly locates the VLP in 95% of the cases, outperforming previous approaches.**

***Index Terms*—Vehicle license plate location; mathematical morphology.**

I. Introduction

An automatic vehicle access control system (AVACS) is an intelligent transportation subsystem, based on image processing and computer vision, that helps in different parking and access tasks, as access authorization control. License plate number is the central information for an AVACS, as it is an unique identifier of a vehicle. The process to automatically define it from digital images can be composed of three steps: vehicle location, VLP location, and VLP recognition.

The VLP location step is typically the less robust and the more computationally intensive. One important factor is image type: in the literature, there are approaches that process binary [1], [2], [3], monochrome (gray-level) [4], [5] or color images [6], and also methods that manipulates different types simultaneously [7]. VLP location based on mathematical morphology [8] usually uses bottom- and top-hat [1] and horizontal gradient [2] operations to highlight VLP saliences (patterns) on the monochrome image. The resulting image is then binarized and morphological operations are applied, trying to keep only the VLP region.

The binarization phase is particularly sensitive: VLP region may be eliminated due to bad binarization threshold estimation. If non-VLP regions are the most highlighted ones, this will cause partial or full VLP region elimination.

We propose a new VLP location method that tackles this problem by delaying the binarization step. It is inspired by an in-depth study of methods in the literature [1], [2], [3], from which it shares some components. First, the horizontal gradient is computed on the original monochrome image and a mean filter is applied on the resulting integer-valued image. The filtered image is processed with morphological operations, with the specific goal to improve binarization, as we will see later. VLP region candidates are identified in the resulting binary image by a connected component analysis. Finally, statistical measures are used to choose the most probable VLP region candidate.

Experiments are carried out using two image databases: 377 images acquired by a digital camera at UFOP campus and the 345 images of Greek vehicles available in [7]. Our method achieved successful VLP location rate of 95% (we also implemented other methods for comparison). Since there are empirical parameters, a 5-fold cross-validation scheme was used to estimate them.

The remainder of this paper is organized as follows. In Section II, the proposed method's steps are presented. Our results and comparisons with results obtained by other methods in the literature are shown in Section III. Finally, in Section IV, we present our conclusions and possible future directions to this work.

II. Proposed method

Our method to solve the VLP location based on digital images uses morphological operations, horizontal gradient, connected component analysis and statistical decision. The main contribution of it is that morphological operations are applied on the horizontal gradient image. Note that horizontal gradient operator is used to detect *vertical edges*. There is a training phase where database images are used to estimate some VLP parameters: plate's height and width, distance between characters, distance between the last letter and first number. We used a 5-fold cross validation scheme to estimate them. The flowchart in Fig. 1 shows method's steps that are detailed in the following subsections.

A. Horizontal Gradient

Our working hypothesis is that, in the image of a vehicle, its front and its rear are mainly composed of horizontal lines [9], while its VLP region has a clear predominance of vertical lines.

During horizontal gradient detection, we obtain the vertical lines from the original image by applying the Sobel operator [8]. Fig. 2(b) shows the resulting image of horizontal gradient detection on the original image in Fig. 2(a).

978-1-4577-0653-0/11/$26.00

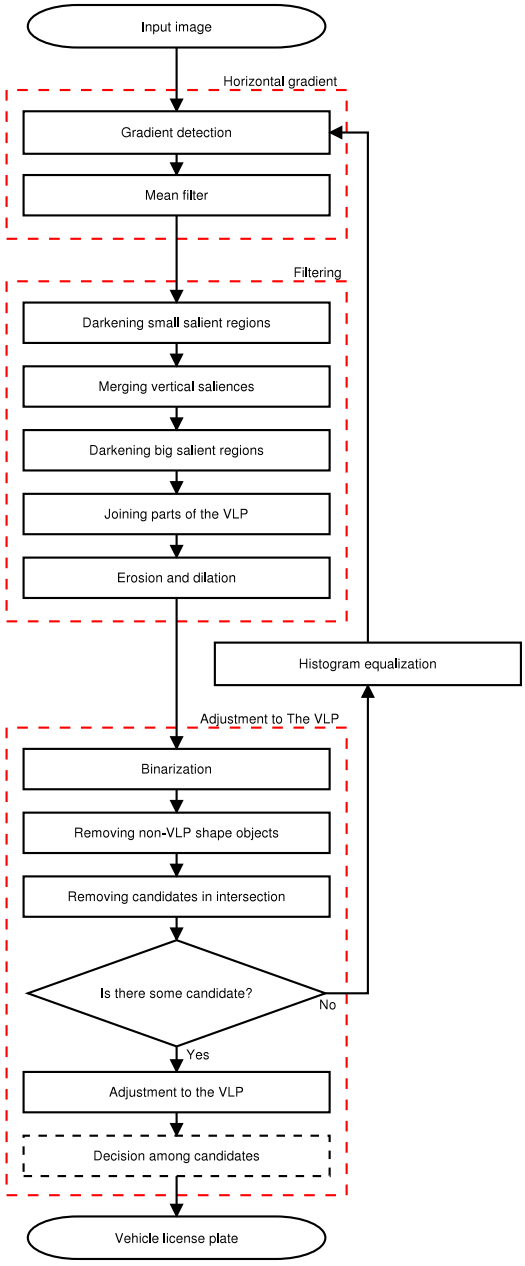

Fig. 1. Steps of the vehicle license plate location method.

A mean filter [3] is applied to the image, in order to have VLP region more emphasized, as we expect it to have a great concentration of high valued pixels. The final image of Horizontal Gradient phase can be seen in Fig. 2(c). Filter's mask is a $\alpha_1\hat{w}_P \times \alpha_1\hat{h}_P$-rectangle, where $\hat{w}_P$ and $\hat{h}_P$ are the expected VLP width and height, respectively, parameters mentioned before.

B. Filtering

At the filtering phase, the goal is to darken every non-VLP region pixel. Morphological operations proposed in [1], [2] are applied to the current *monochrome* image. The strategy is to darken high valued regions (saliences) that don't fit the expected size. We use the aforesaid VLP parameters – minimum character height in pixels (*MINHCHAR*) and maximum character height in pixels (*MAXHCHAR*) – to define the operations' structuring elements (SEs).

Small non-VLP salient regions are darkened by a morphological opening operation with a column SE of size equals to *MINHCHAR* (see Fig. 2(d)). The joint application of mean filter and opening operation causes undesirable variation among pixel values of VLP region though, perceived as gaps between its vertical saliences. We restore smoothness in these values – which is equivalent to replenish the artificial created gaps – using a morphological closing operation with a line SE of size equals to expected inter-character distance VLP parameter.

Big non-VLP salient regions are also darkened by morphological operations. A top-hap operation in an image with a particular SE consists of subtracting the opening image with the SE from the original image. As the opening image's pixel values are less than or equal their corresponding values in the original image, with a column SE of size *MAXHCHAR*, big salient regions will have their pixel's values lowered, that is, they will be obfuscated as shown in Fig. 2(e).

This resulting image may exhibit an unwanted feature: the VLP region between the letters and the numbers may be less salient. As a consequence, the binarization process may perform poorly splitting VLP region into two, preventing VLP location. We rejoin these VLP parts with a closing morphological operation with a line SE of size equals to expected distance in pixels between the last letter and the first digit (another VLP parameter obtained during the training prephase).

We close the Filtering phase by removing saliences in the plate's borders that may appear during the horizontal gradient step if, for instance, the VLP is over a dark part of the vehicle. If these saliences are left, we wouldn't find the tightest boundary of VLP's characters, making later plate identification hard or impossible. We apply an erosion operation followed by a dilation operation, both using line SEs. The SEs' sizes were experimentally defined to be $\alpha_2\hat{w}_P$ and $\alpha_3\hat{w}_P$, respectively.

C. Adjustment to the VLP

The goal of this phase is to generate tight potential VLP regions in a binary image. First, we binarize the image to separate salient regions from the background. Despite the fact that we tried to darken non-VLP salient regions while highlighting VLP region, it is still possible that it is not as emphasized as we wanted and we could miss it during binarization. Otsu's method [10] is employed to automatically define the binarization threshold and minimize the chance of a miss (Fig. 2(g)).

In the connected component analysis, as we know the expected size and shape of a VLP, we remove any region that is not VLP-shaped from the binary image. A region is not VLP-shaped if one of the following happens: a) its height is greater than or equal to its width (disproportion); b) its width is smaller than VLP parameter *MINWCHARS* (small objects);

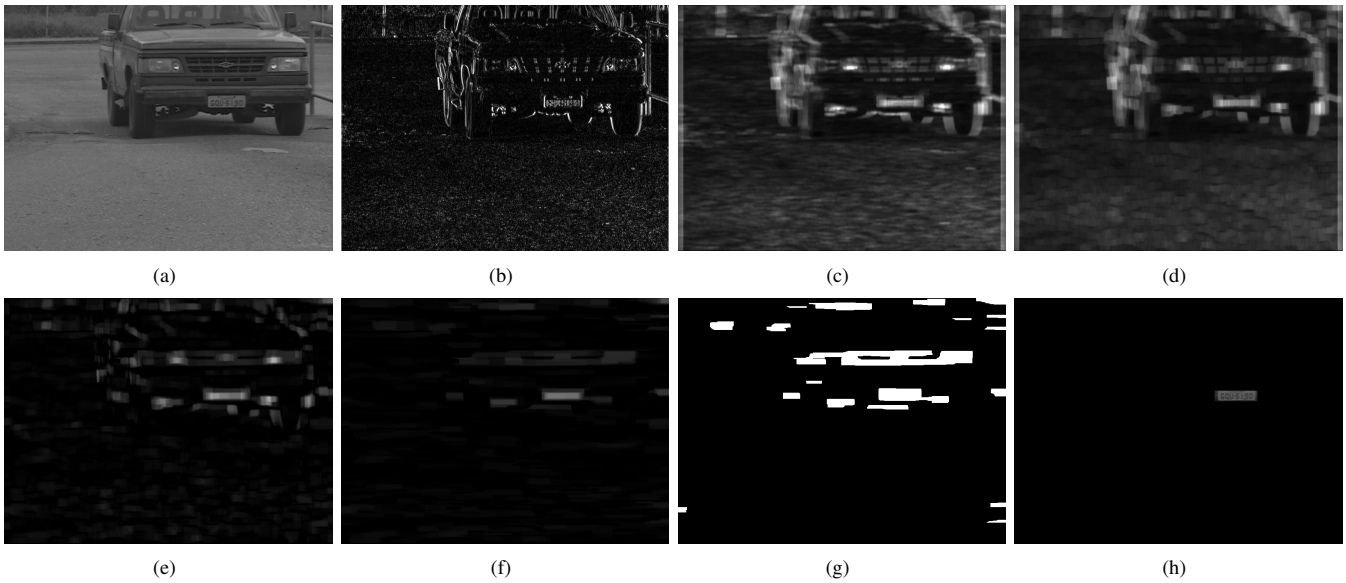

Fig. 2. Steps of the vehicle license plate location method: (a) Original image; (b) Horizontal gradient; (c) Mean filter on horizontal gradient; (d) Small saliences darkened; (e) Big saliences darkened; (f) Erosion and dilation operations; (g) Binarization; (h) Finding the vehicle license plate.

or c) it touches image boundary. Although the VLP can be near to the image margin, after applying the operations of the filtering step (Section II-B), the object referring to the VLP region will not be reaching the image margin.

In the final image, we maintain only objects' bounding boxes, that is, we end up with rectangular objects: the VLP region candidates. Any two intercepting candidates are eliminated based on the fact that VLP is basically composed of vertical edges and the associated candidate(s) does not intercept any other candidate generated by vehicle's horizontal edges. Other vertical edge dominant candidates – like sticker and brand names – are not close enough to the VLP to make their candidates to intercept. On the other hand, candidates originated from background noise – which we do want to eliminate – have a greater chance to touch each other given their random location.

For each remaining candidate, we define a tighter bounding box. First, its initial corresponding bounding box is cut off the monochrome image of the Filtering phase (Section II-B, image in Fig. 2(f)) and is considered as a separated candidate image. A new binarization takes place with Otsu's method. Before, candidate's boundary is expanded to include lower-valued pixels by a dilation operation with a 5×5-square SE, improving threshold estimation. Adopting the same reasoning as in Section II-B, the binary image may contain undesired regions, which are erased by a $\alpha_4 \hat{w}_P$-line-SE erosion operation followed by a $\alpha_5 \hat{w}_P \times \alpha_5 \hat{h}_P$-rectangle-SE dilation. The final candidate bounding box $w_C \times h_C$ is computed as the one that surrounds *all* remaining regions in the resulting image (see the full process in Fig. 3).

The resulting candidate bounding box is checked to see if minimum dimension constraints are satisfied: $w_C \geq$ *MINWCHARS* and $h_C \geq$ *MINHCHAR*, where w_C and h_C stand for the width and height of the bounding box. If they are not, the candidate is discarded, unless it is the single one, in which case the original looser bounding box is kept.

If there is no candidate or all of them are discarded, a histogram equalization is performed in the original image, to get a contrast improvement, and the location process is repeated from its very beginning.

D. Decision among candidates

We expect homogeneousness among pixels' values of the VLP region in the filtered image (Fig. 2(f)). So, we use the coefficient of variation (CV) [11] to measure candidates' quality and to decide among then which is the actual VLP. For every candidate, we take into account only those pixels remaining at the end of the Adjustment to the VLP step. We evaluate the mean and standard deviation values of those pixels in the corresponding image obtained at the end of Filtering step (Section II-B).

The quality measure V of a candidate is defined as:

$$V = \frac{\mu}{CV} = \frac{\mu^2}{\sigma},$$

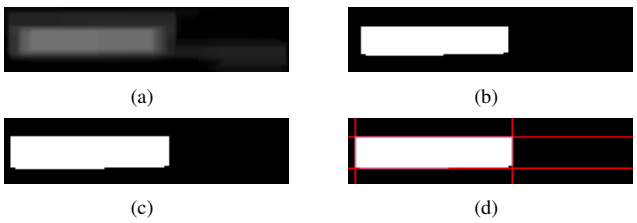

Fig. 3. Operations in a candidate regarding the vehicle license plate: (a) Region corresponding to the image obtained at the end of Section II-B; (b) Region binarization; (c) Erosion and dilation; (d) Bounding box update.

where μ and σ stand for the mean and standard deviation of those pixels' values and the coefficient variation is $CV = \frac{\sigma}{\mu}$.

The candidate with the largest V is chosen as the VLP (Fig. 2(h)). A final dilation by a 7×7-SE is applied to guarantee that no VLP character is (partially) cut off.

III. Results

We carried out tests to compare our method with three other ones [2], [4], [12]. The methods were implemented in MATLAB and the source codes are available in [13]. The runtime of our method is 0.73 ± 0.18 seconds for each image, on an Intel Pentium Dual-Core T2370, 1.73 GHz with 2 GB RAM running Ubuntu Linux 9.10. We believe that an optimized version of the code would be suitable to real-time applications.

A. Validation methodology

Every image in the experiments was manually labeled with its minimum bounding box that includes all VLP characters, *i.e.*, r_{char} (Fig. 4(a)) and its minimum bounding box that includes the entire VLP, *i.e.*, r_{vlp} (Fig. 4(b)). The labeled images are also available in [13].

Results are presented with respect to the located area la and the excessive area ea defined as follows:

$$la = \frac{area(r_{char} \cap r_{met})}{area(r_{char})} \quad (1)$$

$$ea = \frac{area(\overline{r_{vlp}} \cap r_{met})}{area(r_{vlp})} \quad (2)$$

where r_{met} is the region found by the method and $area()$ is a function that obtains the area, in pixels, of a given region.

Experimentally, we determined what is a successful location: it is one with $la \geq 85\%$ and $ea \leq 100\%$. Within the first limit, no VLP character information is lost and within the second, extra pixels do not mess up the recognition.

As some of the implemented methods [4], [12] don't make clear how they choose among candidates, in the results, we considered the best candidate to be the one with the highest la value.

B. Image database

Two image databases are used: 377 images (800×600 pixels), acquired at UFOP campus in order to emulate typical AVACS conditions (Brazilian vehicles), and 345 images (93 of 800×600 pixels and 252 of 640×480 pixels), available in [7] and used for comparison purposes (Greek vehicles).

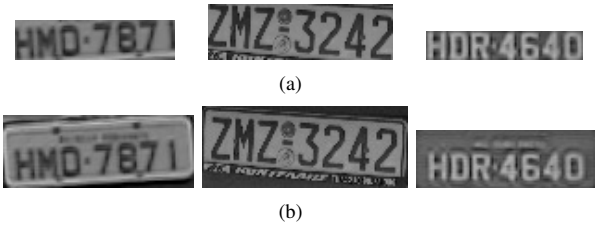

(a)

(b)

Fig. 4. Examples of labeling of images: (a) Minimum bounding box that includes all the characters; (b) Minimum bounding box that includes the entire vehicle license plate.

For the first image database, the expected size for the VLP is 17.60 ± 2.44 tall and 88.21 ± 10.10 wide (based on the image of characters labeled) with minimum and maximum height and width of 13, 28, 73, and 122, respectively. For the Greek image database, the expected size for the VLP is 26.84 ± 6.16 tall and 117.43 ± 22.56 wide with minimum and maximum height and width of 15, 51, 71, and 182, respectively.

MINHCHAR, *MAXHCHAR*, and *MINWCHARS* constant values, 12, 53, and 67, respectively, are closely associated with our method's invariance to scale. The more the first two are spread out, the less accurate we are on VLP salient region detection. If *MINWCHARS* is small, it is probable that the candidate number raises too much and candidate decision is more difficult.

As mentioned before, every VLP parameter of our method were obtained empirically using 5-fold cross-validation scheme. Each partition of the cross-validation technique contains images of the two databases, *i.e.*, the methods were parameterized and executed based on the two image databases. Values for α_1, α_2, α_3, α_4, and α_5 heuristic parameters were setup to 0.20, 0.40, 0.60, 0.05, and 0.10, respectively, using another small database of 10 images.

C. Analysis of results

In Table I, we present the results obtained with the Brazilian images, the Greek images and with all images. The results presented are not considering decision step. That is, the candidate that best fits to the VLP is chosen. We take this decision because two methods [4], [12] do not explain how the decision is made among candidates. From the left to right columns, we show the description, the optimum location ($la > 85\%$ and $ea < 100\%$), the excessive location ($la > 85\%$ and $ea \geq 100\%$), the location error ($la \leq 85\%$ and $ea < 100\%$), the "naïve" location ($la > 0$) rates, and the mean number of candidates generated by each method. Values in the table are obtained by a 5-fold cross-validation scheme, and we present their mean and standard deviation ($\mu \pm \sigma$).

Fig. 6 summarizes the results obtained by each method for each image in graphs of located area versus excessive area.

With the usual "naïve" location metric, our method obtains the highest rates for all databases, but the performance difference is not always statiscally significant. With "optimum" location metric ($la > 85\%$ and $ea < 100\%$), however, which takes location and excessive area tradeoff into account, the values reported in [4], [12] decrease drastically. From this result, we argue that these methods could not become part of an AVACS, since their located VLP would not contain enough information for vehicle identification. Moreover, the number of VLP candidates produced by [12] is significantly bigger than the other methods, what makes candidate selection harder. On the other hand, our method and method [2] generate the smallest number of VLP candidates.

Our method obtains successful VLP optimum location rate of $94.18\% \pm 0.20\%$ ($92.04\% \pm 0.59\%$ and $96.52\% \pm 0.33\%$ for

(a) (b) (c) (d)

Fig. 5. Examples of errors in the location of the vehicle license plate: (a) Location vehicle brand name (decision error); (b) Location of brand symbol (decision error); (c) Location of extra region; (d) Location of only part of vehicle license plate.

TABLE I
RESULTS OBTAINED WITH THE BRAZILIAN, GREEK, AND ALL IMAGE DATABASES.

	optimum location	excessive location	location error	"naïve" location	candidates number
Brazilian database	$la > 85\%$ and $ea < 100\%$	$la > 85\%$ and $ea \geq 100\%$	$la \leq 85\%$ and $ea < 100\%$	$la > 0$	
Suryanarayana *et al.* method ([2])	$93.10\% \pm 1.18\%$	$0.00\% \pm 0.00\%$	$6.37\% \pm 1.05\%$	$94.03\% \pm 1.45\%$	2.14 ± 1.27
Vargas *et al.* method ([4])	$34.74\% \pm 2.03\%$	$13.79\% \pm 0.43\%$	$39.53\% \pm 3.26\%$	$54.64\% \pm 1.97\%$	4.43 ± 4.07
Wang *et al.* method ([12])	$54.63\% \pm 1.78\%$	$17.52\% \pm 1.40\%$	$23.60\% \pm 1.38\%$	$98.14\% \pm 0.40\%$	25.22 ± 10.01
Proposed method	$94.43\% \pm 0.50\%$	$1.59\% \pm 0.55\%$	$2.12\% \pm 0.54\%$	$96.02\% \pm 0.64\%$	2.57 ± 1.75
Greek database	$la > 85\%$ and $ea < 100\%$	$la > 85\%$ and $ea \geq 100\%$	$la \leq 85\%$ and $ea < 100\%$	$la > 0$	
Suryanarayana *et al.* method ([2])	$93.85\% \pm 0.80\%$	$0.87\% \pm 0.19\%$	$5.29\% \pm 0.88\%$	$98.55\% \pm 0.34\%$	3.14 ± 2.48
Vargas *et al.* method ([4])	$64.64\% \pm 1.72\%$	$5.21\% \pm 0.80\%$	$27.11\% \pm 1.92\%$	$86.95\% \pm 1.04\%$	6.41 ± 4.96
Wang *et al.* method ([12])	$62.32\% \pm 0.59\%$	$2.32\% \pm 0.45\%$	$31.59\% \pm 0.66\%$	$95.07\% \pm 0.23\%$	19.41 ± 7.43
Proposed method	$96.52\% \pm 0.18\%$	$0.87\% \pm 0.20\%$	$2.61\% \pm 0.15\%$	$99.13\% \pm 0.19\%$	1.53 ± 1.20
The two database	$la > 85\%$ and $ea < 100\%$	$la > 85\%$ and $ea \geq 100\%$	$la \leq 85\%$ and $ea < 100\%$	$la > 0$	
Suryanarayana *et al.* method ([2])	$93.46\% \pm 0.95\%$	$0.42\% \pm 0.09\%$	$5.85\% \pm 0.94\%$	$96.19\% \pm 0.89\%$	2.62 ± 2.01
Vargas *et al.* method ([4])	$49.03\% \pm 1.80\%$	$9.70\% \pm 0.43\%$	$33.59\% \pm 2.44\%$	$70.08\% \pm 1.46\%$	5.38 ± 4.62
Wang *et al.* method ([12])	$58.31\% \pm 0.90\%$	$10.25\% \pm 0.69\%$	$27.42\% \pm 0.58\%$	$96.68\% \pm 0.22\%$	22.44 ± 9.33
Proposed method	$95.43\% \pm 0.20\%$	$1.25\% \pm 0.33\%$	$2.35\% \pm 0.34\%$	$97.51\% \pm 0.40\%$	2.07 ± 1.60

the Brazilian and Greek databases, respectively) considering our decision algorithm and $95.43\% \pm 0.20\%$ without this decision, exhibiting the best performance among all the methods.

Method [4] is more susceptible to background variations than ours. This is its main source of errors, when vertical and horizontal projections of a preprocessed image are computed, hindering the choice of robust constants.

On the other hand, method [12] is not scale invariant. If its assumption that the plate region has a maximum width (step 6 of [12]) is not respected, the VLP detection (step 7 of [12]) loses its efficacy: as no lateral growth is allowed, a narrow VLP would be missed. As the database contains images where the VLP width varies from 71 to 182 (Section III-B), this may explain its relatively poor performance.

Our method barely fails in deciding among candidates. There are regions in the vehicle (*e.g.*, bus identification number) that may have big horizontal gradients and size close to the VLP size. These regions might be wrongly selected as the VLP region. We present some failure scenarios in Fig. 5.

IV. CONCLUSIONS AND FUTURE WORK

In this paper, we proposed a new VLP location method based on the horizontal gradient, morphological operations on monochrome and binary images, connected component analysis, and statistical measures. As other gradient-based methods, our approach is sensitive to light changes and noise, as depicted in Figure 5(d). VLP was only partially located due to a shadow region. On the other had, our method is scale invariant, as long as VLP dimensions fall into a prespecified (sparse) range. In average, we obtained a successful VLP location rate of 95%, outperforming previous methods in both databases, which have very different characteristics.

We also introduced a methodology to statistically evaluate the located VLPs' quality. With that, we are able to quantitatively compare methods in the literature.

The methods presented in the literature for VLP location use the assumption that the vehicle is presented in the image to be processed. We consider an AVACS as a system composed of vehicle tracking and location from video, then VLP location, and finally VLP character recognition.

The use of vehicle tracking videos can enhance our method's robustness to scale changes, as we can obtain vehicle's width in pixels. The VLP parameters could be better estimated having this width information. In addition to that, with multiple frames, we can define the one which best represents the vehicle and its VLP.

Another straightforward improvement is adding VLP character recognition phase to the method. The decision among

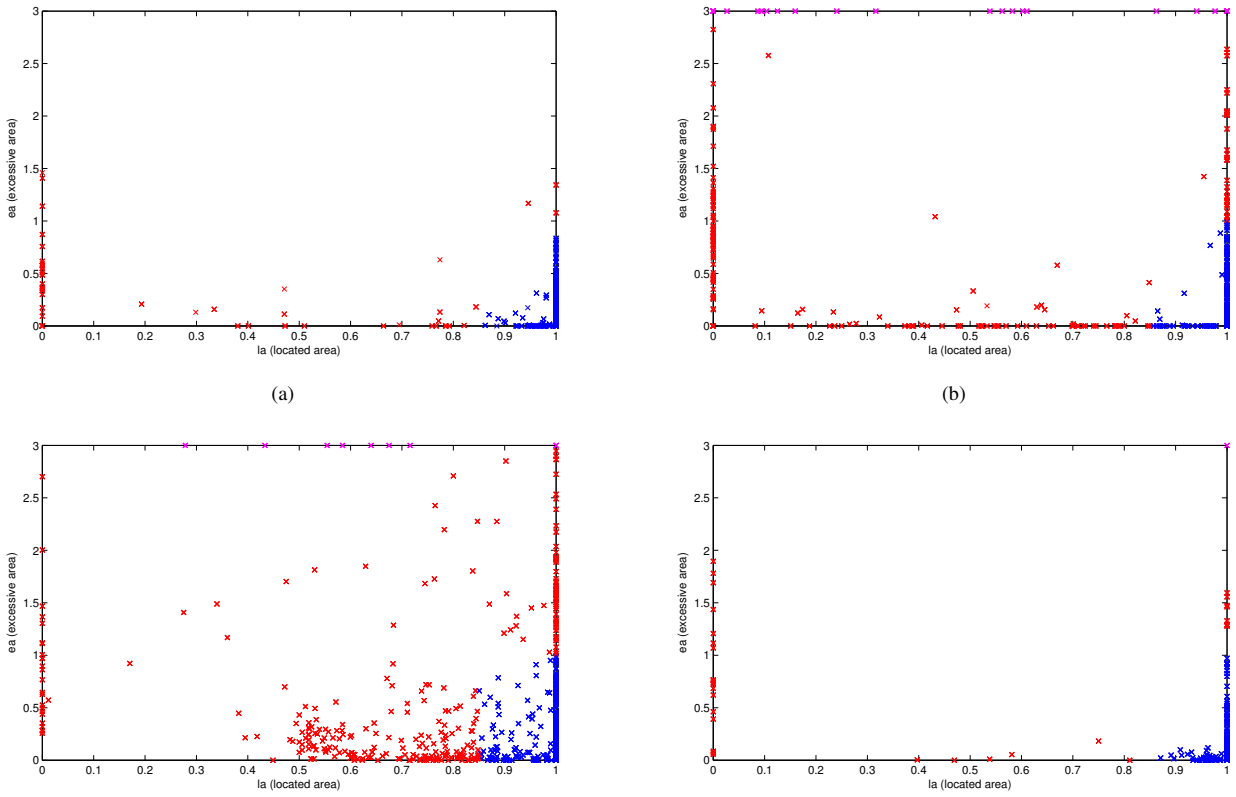

Fig. 6. Results (located area × excessive area): (a) Suryanarayana *et al.* method [2]; (b) Vargas *et al.* method [4]; (c) Wang *et al.* method [12]; (d) Proposed method.

candidates would be more accurate with this extra information. Both features would bring our method closer to a full AVACS.

ACKNOWLEDGMENT

The authors would like to thank the PIP/UFOP (Program for Initiation in Research of UFOP) for the scholarship granted for this work.

REFERENCES

[1] F. Martín, M. García, and J. L. Alba, "New methods for automatic reading of VLP's (Vehicle License Plates)," in *Proceedings of IASTED International Conference on Signal Processing, Pattern Recognition, and Applications (SPPRA)*, Jun. 2002, pp. 84–87.

[2] P. V. Suryanarayana, S. K. Mitra, A. Banerjee, and A. K. Roy, "A morphology based approach for car license plate extraction," in *Proceedings of the IEEE INDICON*, Dec. 2005, pp. 24–27.

[3] B. Hongliang and L. Changping, "A hybrid license plate extraction method based on edge statistics and morphology," in *Proceedings of the International Conference on Pattern Recognition (ICPR)*, vol. 2, Aug. 2004, pp. 831–834.

[4] M. Vargas, S. L. Toral, F. Barrero, and F. Cortés, "A license plate extraction algorithm based on edge statistics and region growing," in *Proceedings of the International Conference on Image Analysis and Processing (ICIAP)*, vol. 5716, Aug. 2009, pp. 317–326.

[5] V. Abolghasemi and A. Ahmadyfard, "An edge-based color-aided method for license plate detection," *Image and Vision Computing (IVC)*, vol. 27, no. 8, pp. 1134–1142, Jul. 2009.

[6] S.-L. Chang, L.-S. Chen, Y.-C. Chung, and S.-W. Chen, "Automatic license plate recognition," *Intelligent Transportation Systems (ITS), IEEE Transactions on*, vol. 5, no. 1, pp. 42–53, Mar. 2004.

[7] C.-N. E. Anagnostopoulos, I. E. Anagnostopoulos, I. D. Psoroulas, V. Loumos, and E. Kayafas, "License plate recognition from still images and video sequences: A survey," *Intelligent Transportation Systems (ITS), IEEE Transactions on*, vol. 9, no. 3, pp. 377–391, Sep. 2008.

[8] R. C. Gonzalez and R. E. Woods, *Digital Image Processing*, 3rd ed. Prentice Hall, 2007.

[9] M. Sarfraz, M. J. Ahmed, and S. A. Ghazi, "Saudi arabian license plate recognition system," in *Proceedings of the International Conference on Geometric Modeling and Graphics (GMAG)*, Jul. 2003, pp. 36–41.

[10] N. Otsu, "A threshold selection method from gray-level histograms," *Systems, Man, and Cybernetics (SMC), IEEE Transactions on*, vol. SMC-9, pp. 62–66, Jan. 1979.

[11] D. C. Montgomery and G. C. Runger, *Applied Statistics and Probability for Engineers*, 3rd ed. John Wiley & Sons, Inc., 2003.

[12] Y.-R. Wang, W.-H. Lin, and S.-J. Horng, "A sliding window technique for efficient license plate localization based on discrete wavelet transform," *Expert Systems with Applications (ESWA)*, vol. 38, no. 4, pp. 3142–3146, Apr. 2011.

[13] P. R. Mendes-Júnior, D. Menotti, J. M. R. Neves, and A. I. Tavares, "Vehicle license plate location (VLPL) algorithms." [Online]. Available: https://github.com/pedrormjunior/vlpl